$B_5H_{12}^-$,[38] $B_5H_9{\cdot}L_2$ (L = NR_3 or PR_3),[39,40] $B_5H_9{\cdot}L$ (L = dppm, dppe, tmeda, etc.),[41,42] $B_3H_5{\cdot}3PMe_3$,[40b,43] $Me_3NCB_5H_{11}$,[44] $B_4H_8{\cdot}PR_3$,[45] $B_4H_8{\cdot}$tmeda,[46] and $B_7H_{12}Fe(CO)_4^-$.[47] The isolation of II suggests that a variety of larger cage hypho cluster systems are possible based on the S_2B_7 cage system, and indeed, recent work in our laboratory has already resulted in the synthesis of a number of eight- and nine-vertex hypho clusters.[48]

The fact that II contains three open faces suggests that it may also serve as a versatile starting material for the construction of new hybrid clusters in which various heteroatoms can be inserted into these faces. Of particular interest is the 5-fold face B2, B8, S14, B12, S7, which contains the boron–boron-bridging hydrogen. If the bridging proton is removed, then a pentagonal face is generated with a formal −1 charge. This would be a direct analogue of a $C_5H_5^-$ ligand; however, because the B–S distances in the ring (~1.90–1.96 Å) are longer than the C–C distances in a cyclopentadienyl ring (average C–C ≈ 1.4 Å), the thiaborane ring is larger. Thus, the distances across the face, S7–S14 = 3.24 Å and B2–B12 = 3.01 Å, are considerably longer than the ~2.3 Å observed between nonadjacent carbons in a cyclopentadienyl ring. This difference in size may result in unique bonding abilities.

IV is one of the few members of the tricarbon carborane series, the only others being *nido*-$C_3B_3H_7$,[49] *closo*-$C_3B_5H_7$,[50] and the recently reported *nido*-5,6,10-$Me_3C_3B_7H_8$,[20] and is the only such compound to have a CH_2 cage vertex. Given the few compounds in this series and the absence of efficient synthetic routes, the chemistry of this carborane class has not yet been extensively developed. IV is now the most available tricarbon carborane and may serve as both a useful precursor to other such carboranes and as a starting material for the construction of new heteroatom cluster systems.

Acknowledgment. We thank the National Science Foundation for the support of this research. We also thank Dr. Robert Williams for his comments concerning the structure of II.

Supplementary Material Available: Tables of anisotropic temperature factors, hydrogen atom coordinates, bond angles, and least-squares planes (4 pages); a listing of observed and calculated structure factor amplitudes (3 pages). Ordering information is given on any current masthead page.

(38) Remmel, R. J.; Johnson, H. D., II; Jaworiwsky, I. S.; Shore, S. G. *J. Am. Chem. Soc.* **1975**, *97*, 5395–5403.
(39) (a) Burg, A. B. *J. Am. Chem. Soc.* **1957**, *79*, 2129–2132. (b) Savory, C. G.; Wallbridge, M. G. H. *J. Chem. Soc., Dalton Trans.* **1973**, 179–184.
(40) (a) Fratini, A. V.; Sullivan, G. W.; Denniston, M. L.; Hertz, R. K.; Shore, S. G. *J. Am. Chem. Soc.* **1974**, *96*, 3013–3015. (b) Kameda, M.; Kodama, G. *Inorg. Chem.* **1980**, *19*, 2288–2292.
(41) Alcock, N. W.; Colquhoun, H. M.; Haran, G.; Sawyer, J. F.; Wallbridge, M. G. H. *J. Chem. Soc., Chem. Commun.* **1977**, 368–370.
(42) Miller, N. E.; Miller, H. C.; Muetterties, E. L. *Inorg. Chem.* **1964**, *3*, 866–869.
(43) Hertz, R. K.; Denniston, M. L.; Shore, S. G. *Inorg. Chem.* **1978**, *17*, 2673–2674.
(44) Duben, J.; Heřmánek, S.; Štíbr, B. *J. Chem. Soc., Chem. Commun.* **1978**, 287.
(45) Kodama, G.; Kameda, M. *Inorg. Chem.* **1979**, *18*, 3302–3306.
(46) (a) Colquhoun, H. M. *J. Chem. Res.* **1978**, 451. (b) Alcock, N. W.; Colquhoun, H. M.; Haran, G.; Sawyer, J. F.; Wallbridge, M. G. H. *J. Chem. Soc., Dalton Trans.* **1982**, 2243–2255.
(47) (a) Hollander, O.; Clayton, W. R.; Shore, S. G. *J. Chem. Soc., Chem. Commun.* **1974**, 604–605. (b) Mangion, M.; Clayton, W. R.; Hollander, O.; Shore, S. G. *Inorg. Chem.* **1977**, *16*, 2110–2114.
(48) Kang, S. O.; Sneddon, L. G. *J. Am. Chem. Soc.*, in press.
(49) (a) Bramlett, C. L.; Grimes, R. N. *J. Am. Chem. Soc.* **1966**, *88*, 4269–4270. (b) Grimes, R. N.; Bramlett, C. L. *J. Am. Chem. Soc.* **1967**, *89*, 2557–2560. (c) Grimes, R. N.; Bramlett, C. L.; Vance, R. L. *Inorg. Chem.* **1968**, *7*, 1066–1070. (d) Howard, J. W.; Grimes, R. N. *J. Am. Chem. Soc.* **1969**, *91*, 6499–6500. (e) Franz, D. A., Jr.; Howard, J. W.; Grimes, R. N. *J. Am. Chem. Soc.* **1969**, *91*, 4010–4011. (f) Howard, J. W.; Grimes, R. N. *Inorg. Chem.* **1972**, *11*, 263–267.
(50) Thompson, M. L.; Grimes, R. N. *J. Am. Chem. Soc.* **1971**, *93*, 6677–6679.

Contribution from the Department of Chemistry, Massachusetts Institute of Technology, Cambridge, Massachusetts 02139

Complexes of Rhenium Carbonyl Containing Ferrocenyl-Derived Ligands: Tunable Electron Density at Rhenium by Control of the Redox State of the Ferrocenyl Ligand

Timothy M. Miller, Kazi J. Ahmed, and Mark S. Wrighton*

Received October 17, 1988

The new complexes $(Fe(C_5H_4PPh_2)_2)Re(CO)_3Cl$, *cis*-$(FcPPh_2)Re(CO)_4Cl$, *fac*-$(FcPPh_2)_2Re(CO)_3Cl$, *fac*-$(FcPy)_2Re(CO)_3Cl$, and $FcRe(CO)_5$ (Fc = ferrocenyl; Py = 4-pyridyl) have been synthesized and characterized for the purpose of investigating the tunability of the electron density on Re by changes in the redox state of the ferrocene center(s). The structures of $(Fe(C_5H_4PPh_2)_2)Re(CO)_3Cl$ and *fac*-$(FcPPh_2)_2Re(CO)_3Cl$ were solved by X-ray crystallography. Structural parameters: for $(Fe(C_5H_4PPh_2)_2)Re(CO)_3Cl$, a = 11.650 (2) Å, b = 19.534 (5) Å, c = 14.318 (2) Å, β = 93.76 (1)°, V = 3251 (2) Å^3, Z = 4, space group $P2_1/c$, R_1 = 0.032, R_2 = 0.033; for *fac*-$(FcPPh_2)_2Re(CO)_3Cl$, a = 11.859 (2) Å, b = 20.105 (4) Å, c = 17.060 (3) Å, β = 92.26 (1)°, V = 4064 (2) Å^3, Z = 4, space group $P2_1/c$, R_1 = 0.049, R_2 = 0.049. All of the complexes exhibit ferrocene-based, reversible oxidations. The oxidized complexes were prepared in situ, either by electrolysis in a spectroelectrochemical cell or by chemical oxidation, and characterized by spectroscopic methods (IR and UV/vis) and by reduction back to the neutral complexes. The carbonyl stretching frequencies in all of the complexes shift to higher energy upon oxidation. The magnitudes of the shifts range from 12–33 cm^{-1} for $FcRe(CO)_5$ to 4–7 cm^{-1} for $(FcPy)_2Re(CO)_3Cl$ and are closely related to the number of bonds separating the ferrocene moiety and the Re atom.

We wish to report the synthesis, characterization, and properties of the Re carbonyl complexes shown in Scheme I, all of which have ligands derived from ferrocene. We are interested in organometallic complexes having pendant redox-active ligands, because changing the oxidation state of a pendant ligand should change the spectroscopic properties and reactivity of the metal in such complexes without changing the immediate coordination sphere. Numerous series of complexes have been studied where systematic changes in the ligand, e.g. C_5H_5 vs C_5Me_5, have profound effects on the spectroscopic properties and reactivity of the metal center.[1-3] In such situations, changes in chemical properties often stem from a combination of electronic and steric effects. Tuning of electron density in the central metal of a

* To whom correspondence should be addressed.

(1) Bitterwolf, T. E. *Polyhedron* **1988**, *7*, 409–415.
(2) Box, J. W.; Gray, G. M. *Inorg. Chem.* **1987**, *26*, 2774–2778.
(3) Tolman, C. A. *Chem. Rev.* **1977**, *77*, 313–348.

0020-1669/89/1328-2347$01.50/0

Scheme I. Ferrocenyl–Rhenium Complexes Studied in This Work

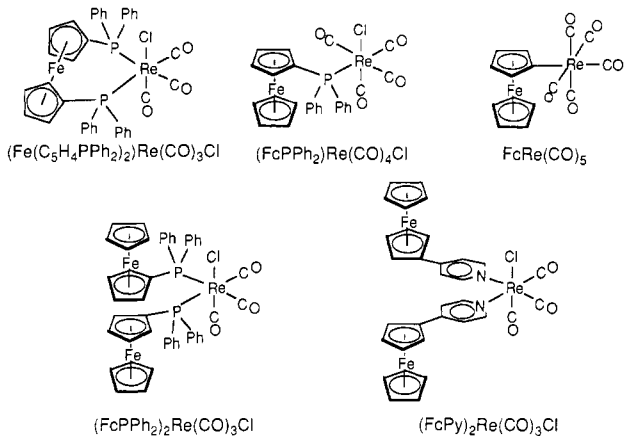

complex without changing the coordination sphere offers the prospect of rational control of reactivity. In this work we establish that spectroscopic properties of the Re carbonyl species shown in Scheme I can be varied by changing the oxidation state of a pendant ferrocenyl ligand. The magnitude of the changes varies with structure. We chose ferrocene-based ligands, because ferrocene-centered oxidations should be reversible.[4] We chose the Re species, because the synthetic chemistry is simple, Re-centered oxidations are difficult, and the complexes are generally substitutionally inert.[5,6] Metal carbonyls are useful in assessing consequences of changes in the ferrocene redox state because M–CO stretching frequencies depend on the electron density at the metal center.[7]

We are not the first to observe changes in CO stretching frequencies in a metal complex upon oxidation of a ferrocene-derived ligand.[8] Kotz et al. prepared ferrocenylphosphines (Fc_nPPh_{3-n}, n = 1–3) and observed small shifts (~5 cm^{-1} per oxidized ferrocene) to higher energy in the peak positions of the E/A_1' IR bands upon oxidation of the ferrocene(s) in complexes of $W(CO)_5$ and $Mo(CO)_5$.[9,10] In a related vein, Davison et al. observed that the W–CO bands in $(Co(C_5H_4PPh_2))W(CO)_4^+$ occur at higher energy than those for $(Fe(C_5H_4PPh_2)_2)W(CO)_4$.[11] Two recent publications demonstrate that oxidation of ferrocenyl ligands attached to triosmium or tricobalt clusters shifts the M–CO bands to higher energies.[12,13] There are also many examples of spectroscopic property and reactivity changes induced in a metal center by reduction of a pendant redox-active ligand.[14,15]

Table I. IR and UV/Vis Band Positions and Molar Absorptivities for Neutral and Oxidized Ferrocenyl–Rhenium Complexes

complex	IR bands ν_{CO} (ϵ)[a]	UV/vis bands λ_{max} (ϵ)[b]
$FcRe(CO)_5$	2132 (700), 2049 (190), 2016 (10000), 1982 (2200)	376 (1100), 480 (320)
$FcRe(CO)_5^+$	2144 (980), 2076 (360), 2030 (8800), 2015 (2900)	400 (1400), 702 (440)
$(Fe(C_5H_4PPh_2)_2)$-$Re(CO)_3Cl$	2035 (3250), 1953 (1910), 1900 (1710)	436 (159)
$(Fe(C_5H_4PPh_2)_2)$-$Re(CO)_3Cl^+$	2047 (3400), 1972 (1700), 1920 (1800)	495 (270), 620 (150)
$(FcPPh_2)Re(CO)_4Cl$	2107 (990), 2013 (2500), 2003 (3000), 1941 (1630)	314 (2900), 340 (1600), 456 (228)
$(PPh_3)Re(CO)_4Cl$[c]	2100, 2015, 1998, 1940	
$(FcPPh_2)Re(CO)_4Cl^+$	2110 (1200), 2024 (1700), 2005 (3300), 1961 (1600)	642 (440)
$(FcPy)_2Re(CO)_3Cl$[d]	2022 (4950), 1915 (3430), 1888 (2710)	476 (3350)
$(FcPy)_2Re(CO)_3Cl^{2+}$[d]	2026 (4500), 1922 (3100), 1894 (2600)	684 (700)
$(FcPPh_2)_2Re(CO)_3Cl$	2031 (3000), 1946 (1900), 1898 (1540)	458 (443)
$(FcPPh_2)_2Re(CO)_3Cl^{2+}$	2039 (2400), 1956 (1600), 1914 (1400)	622 (600)
$(FcPPh_2)_2Re(CO)_3Cl^+$	2036, 1951, 1907	

[a] Band positions are in wavenumbers (cm^{-1}) and molar absorptivities have the units M^{-1} cm^{-1}. All IR spectra were measured at room temperature in CH_2Cl_2 unless noted otherwise. [b] Band positions are in nm and molar absorptivities have the units M^{-1} cm^{-1}. UV/vis spectra of neutral complexes were measured in CH_2Cl_2 at room temperature unless noted otherwise. UV/vis spectra of oxidized complexes were measured in CH_2Cl_2/0.1 M $[n\text{-}Bu_4N]ClO_4$ at room temperature unless noted otherwise. [c] These data are from ref 22. [d] IR and UV/vis spectra were measured in CH_3CN at room temperature for these complexes. The UV/vis spectrum of $(FcPy)_2Re(CO)_3Cl^{2+}$ was measured in CH_3CN/0.1 M $[n\text{-}Bu_4N]ClO_4$.

Experimental Section

General Data. CH_2Cl_2 and CH_3CN were distilled from CaH_2 prior to use in chemical oxidations or spectroelectrochemical experiments. The electrolytes $[n\text{-}Bu_4N]ClO_4$ and $[Et_4N]PF_6$ were recrystallized from EtOH prior to use. Benzoquinone and ferrocene were also recrystallized from EtOH prior to use. All other reagents and starting materials were used as received.

NMR spectra were measured on WM 270, WM 250, and Varian 300 instruments. FTIR spectra were measured on Nicolet 7100 and 60SX spectrometers. UV/vis spectra were recorded on a Hewlett Packard 8451A diode array spectrometer. Molar absorptivities were determined in IR, spectroelectrochemical, or UV/vis cells of known path length by using solutions whose concentrations were accurately known. Mass spectra were measured on a Finnigan MAT System 8200 spectrometer. Elemental analyses were obtained from Galbraith Laboratories or Atlantic Microlab Inc.

Synthesis of Complexes. Diphenylferrocenylphosphine,[16] bromoferrocene,[17] diferrocenylmercury[18] and (dppe)$Re(CO)_3Cl$ (dppe = bis(diphenylphosphino)ethane)[19] were prepared by literature procedures.

4-Ferrocenylpyridine. Ferrocenylmagnesium bromide was prepared by a modification of the literature procedure.[20] A 50-mL round-bottomed flask equipped with an Ar inlet, condenser, rubber septum, and magnetic stirring bar was charged with 0.39 g (16 mmol) of Mg and placed under an atmosphere of Ar. Et_2O (5 mL) was added to the Mg, and a solution of 1.06 g (4.0 mmol) of bromoferrocene and 0.68 mL (7.9 mmol) of 1,2-dibromoethane in 10 mL of Et_2O was added slowly to the reaction flask. The Et_2O refluxed on its own during the addition, and considerable gas evolved. After completion of the addition, the reaction mixture separated into two layers. The Grignard reagent was used in the next step without isolation.

An aqueous solution of 4-bromopyridine hydrochloride (Aldrich) was made basic with 1 M NaOH and extracted three times with Et_2O. The ethereal solution was washed with saturated aqueous NaCl, dried over

(4) Connelly, N. G.; Geiger, W. E. *Adv. Organomet. Chem.* **1984**, *23*, 1–94.
(5) Bond, A. M.; Colton, R.; McDonald, M. E. *Inorg. Chem.* **1978**, *17*, 2842–2847.
(6) Luong, J. C.; Faltynek, R. A.; Wrighton, M. S. *J. Am. Chem. Soc.* **1980**, *102*, 7892–7900.
(7) Cotton, F. A.; Wilkinson, G. *Advanced Inorganic Chemistry*; Wiley: New York, 1980; p 1072. Collman, J. P.; Hegedus, L. S.; Norton, J. R.; Finke, R. G. *Principles and Applications of Organotransition Metal Chemistry*; University Science Books: Mill Valley, CA, 1987; p 114.
(8) The M–CO peak positions shift to higher energy by 10–30 cm^{-1} upon air oxidation of the Cr atom in the chelating ligand of the complexes $(Cr(C_6H_5PPh_2)_2)M(CO)_4$ (M = Cr, Mo, W). Elschenbroich, C.; Stohler, F. *Angew. Chem., Int. Ed. Engl.* **1975**, *14*, 174–176.
(9) Kotz, J. C.; Nivert, C. L. *J. Organomet. Chem.* **1973**, *52*, 387–406.
(10) Kotz, J. C.; Nivert, C. L.; Lieber, J. M.; Reed, R. C. *J. Organomet. Chem.* **1975**, *91*, 87–95.
(11) Rudie, A. W.; Lichtenberg, D. W.; Katcher, M. L.; Davison, A. *Inorg. Chem.* **1978**, *17*, 2859–2863.
(12) The Co–CO bands shift to higher energy by 12–21 cm^{-1} upon oxidation of the ferrocene in $FcCCo_3(CO)_9$: Colbran, S. B.; Robinson, B. H.; Simpson, J. *Organometallics* **1983**, *2*, 943–951.
(13) The Os–CO bands shift to higher energy by 6–12 cm^{-1} in $Os_3H(FcCO)(CO)_{10}$: Arce, A. J.; Bates, P. A.; Best, S. P.; Clark, R. J. H.; Deeming, A. J.; Hursthouse, M. B.; McQueen, R. C. S.; Powell, N. I. *J. Chem. Soc., Chem. Commun.* **1988**, 478–480.
(14) Creager, S. E.; Murray, R. W. *Inorg. Chem.* **1987**, *26*, 2612–2618. Rieke, R. D.; Henry, W. P.; Arney, J. S. *Inorg. Chem.* **1987**, *26*, 420–427. Kadish, K. M.; Tabard, A.; Zrineh, A.; Ferhat, M.; Guiland, R. *Inorg. Chem.* **1987**, *26*, 2459–2466.
(15) The Re–CO bands shift to lower energy by 12–20 cm^{-1} per electron in the reduction of $(4\text{-benzoylpyridine})_2Re(CO)_3Cl$: Shu, C.-F.; Wrighton, M. S. *Inorg. Chem.* **1988**, *27*, 4326–4329.
(16) Sollot, G. P.; Mertwoy, H. E.; Portnoy, S.; Snead, J. L. *J. Org. Chem.* **1962**, *28*, 1090–1094.
(17) Fish, R. W.; Rosenblum, M. *J. Org. Chem.* **1965**, *30*, 1253–1255.
(18) Roling, P. V.; Roling, S. B.; Rausch, M. D. *Synth. Inorg. Met.-Org. Chem.* **1971**, *1*, 97–102.
(19) Zingales, F.; Graziani, M.; Faraone, F.; Belluco, U. *Inorg. Chim. Acta* **1967**, *1*, 172–176.
(20) Schechter, H.; Helling, J. F. *J. Org. Chem.* **1961**, *26*, 1034–1037.

$MgSO_4$, and concentrated to a clear oil of 4-bromopyridine by rotary evaporation. A solution of the 4-bromopyridine (0.41 g, 2.6 mmol) in 10 mL of Et_2O was prepared under Ar and added to a 100-mL round-bottom flask, equipped with a magnetic stirring bar, condenser, Ar inlet, and rubber septum, containing 16.6 mg (31 μmol) of *cis*-(1,3-bis(diphenylphosphino)propane)dichloronickel under Ar.[21] Both layers of the solution of ferrocenylmagnesium bromide in Et_2O were added to the reaction vessel and the reaction mixture was stirred and refluxed over night. Unreacted Grignard reagent was destroyed by slow addition of H_2O (25 mL). The two-phase reaction mixture was poured into a separatory funnel, and the aqueous phase was washed twice with 25 mL of Et_2O. The combined organic solutions were washed with brine, dried over $MgSO_4$, and concentrated by rotary evaporation. The crude mixture of ferrocenylpyridine and ferrocene was chromatographed on 30 g of silica gel by using 5% MeOH in ether. 4-Ferrocenylpyridine was isolated in 82% yield as a yellow, crystalline solid, mp 136–138 °C. ^{1}H NMR ($CDCl_3$): δ 8.47 (d, 7 Hz, 2 H), 7.33 (d, 7 Hz, 2 H), 4.73 (m, 2 H), 4.43 (m, 2 H), 4.03 (s, 5 H). ^{13}C NMR ($CDCl_3$): δ 149.8, 148.6, 120.6, 81.1, 70.2, 69.9, 66.8. Anal. Calcd for $C_{15}H_{13}NFe$: C, 68.47; H, 4.98; N, 5.32. Found: C, 68.45; H, 5.24; N, 5.19.

Substitution reactions on $Re(CO)_5Cl$ in toluene or chloroform provided the complexes $(Fe(C_5H_4PPh_2)_2)Re(CO)_3Cl$, $(FcPy)_2Re(CO)_3Cl$, $(FcPPh_2)Re(CO)_4Cl$, and $(FcPPh_2)_2Re(CO)_3Cl$.[22,23] Reaction of 1 and 2 equiv of $FcPPh_2$ with $Re(CO)_5Cl$ provided mainly $(FcPPh_2)Re(CO)_4Cl$ and $(FcPPh_2)_2Re(CO)_3Cl$. The complexes were purified by column chromatography on silica gel using 2:1 CH_2Cl_2/hexane. Three equivalents of 4-ferrocenylpyridine were reacted with 1 equiv of $Re(CO)_5Cl$. The product and excess ligand were separated by column chromatography on silica gel using Et_2O. A representative procedure is described and analytical data are provided for the other complexes. Analytical samples of the complexes were prepared by recrystallization from CH_2Cl_2/hexane. Spectroscopic (IR and UV/vis) data are provided in Table I.

***cis*-(Ferrocenyldiphenylphosphine)tetracarbonylchlororhenium.** A 250-mL round-bottom flask equipped with a magnetic stirring bar, condenser, Ar inlet, and rubber septum was charged with $FcPPh_2$ (0.37 g, 1.0 mmol) and $Re(CO)_5Cl$ (0.36 g, 1.0 mmol) and was placed under Ar. $CHCl_3$ (100 mL), which had been deoxygenated with a stream of Ar, was added to the flask, and the solution was refluxed overnight while a slow stream of Ar was passed over the reaction mixture to remove displaced CO. The reaction mixture was concentrated by rotary evaporation and chromatographed on 40 g of silica gel eluting with 2:1 CH_2Cl_2/hexane. A yellow, crystalline solid was obtained weighing 0.57 g (81%). Recrystallization of this complex from several solvents (hexane, CH_2Cl_2/hexane, EtOH, methylcyclohexane) always resulted in material that contained one molecule of solvent for every three to five molecules of complex. Recrystallization from hexane resulted in a solvate containing one molecule of hexane/5.1 molecules of complex, mp 160–165 °C dec. ^{1}H NMR ($CDCl_3$): δ 7.63 (m, 4 H), 7.47 (m, 6 H), 4.57 (s, 2 H), 4.40 (s, 2 H), 4.02 (s, 5 H), 1.27 (s, 0.059 H), 0.87 (t, 0.050 H). ^{31}P NMR ($CDCl_3$): δ −5.57. Anal. Calcd for $C_{26}H_{19}ClFeO_4PRe{\cdot}0.20C_6H_{14}$: C, 45.28; H, 3.04; Cl, 4.92; P, 4.30. Found: C, 45.29; H, 2.95; Cl, 5.01; P, 4.44. Mass spectrum: *m/e* (relative intensity), 704 (1.0), 676 (1.9), 371 (28), 370 (100), 293 (69); M^+ 703.9619 (calcd), 703.9616 (obsd).

***fac*-Bis(diphenylferrocenylphosphine)tricarbonylchlororhenium.** Mp: 198–202 °C dec. ^{1}H NMR ($CDCl_3$): δ 7.67 (m, 4 H), 7.40 (m, 3 H), 7.27 (m, 5 H), 7.10 (m, 8 H), 4.37 (s, 4 H), 4.00 (s, 11 H), 3.90 (s, 3 H). ^{31}P NMR ($CDCl_3$): δ 2.27. Anal. Calcd for $C_{47}H_{38}Fe_2O_3P_2Re$: C, 53.96; H, 3.66; P, 5.92; Cl, 3.39. Found: C, 53.81; H, 3.79; P, 5.86; Cl, 3.79.

***fac*-(1,1′-Bis(diphenylphosphino)ferrocene)tricarbonylchlororhenium.** Mp: 210–240 °C dec. ^{1}H NMR ($CDCl_3$): δ 7.73 (m, 8 H), 7.40 (m, 12 H), 4.93 (s, 2 H), 4.37 (s, 2 H), 4.33 (s, 4 H). ^{31}P NMR ($CDCl_3$): δ 2.8. Anal. Calcd for $C_{37}H_{28}ClFeP_2O_3Re$: C, 51.67; H, 3.28; Cl, 4.12. Found: C, 51.43; H, 3.33; Cl, 4.15.

***fac*-Bis(4-ferrocenylpyridine)tricarbonylchlororhenium.** Mp: 242 °C dec. ^{1}H NMR ($CDCl_3$): δ 8.57 (d, 7 Hz, 4 H), 7.28 (d, 7 Hz, 4 H), 4.73 (s, 4 H), 4.53 (s, 4 H), 4.08 (s, 10 H). ^{13}C NMR ($CDCl_3$): δ 195.7, 192.8, 152.9, 152.7, 121.7, 78.6, 71.5, 70.3, 67.3. Anal. Calcd for $C_{33}H_{26}ClFeN_2O_3Re$: C, 47.64; H, 3.15; Cl, 4.26; N, 3.36. Found: C, 47.47; H, 3.14; Cl, 4.52; N, 3.39.

Ferrocenylpentacarbonylrhenium. We used a procedure similar to a published procedure for the preparation of $PhRe(CO)_5$.[24] A quartz Schlenk tube was charged with a solution of 30.9 mg (54.1 μmol) of Fc_2Hg and 17.2 mg (26.4 μmol) of $Re_2(CO)_{10}$ in C_6H_6 (75 mL) prepared under Ar. The solution was irradiated with a low-pressure Hg lamp (UVP Inc.) for 1 h. Two additional batches were irradiated in the same manner and the resulting solutions combined and concentrated by rotary evaporation. The crude yellow solid was chromatographed on 20 g of silica gel by using *n*-hexane as the eluent. A yellow solid weighing 19.2 mg (21%) was isolated, mp 76–84 °C dec. ^{1}H NMR ($CDCl_3$): δ 4.27 (s, 2 H), 4.10 (s, 5 H), 4.00 (s, 2 H). ^{13}C NMR ($CDCl_3$): δ 183.0, 180.6, 81.8, 70.3, 69.6, 67.9. Mass spectrum: *m/e* (relative intensity), 513 (11), 512 (59), 511 (7), 510 (38), 484 (66), 456 (50), 428 (74), 400 (53), 372 (94), 370 (100); M^+ 511.9356 (calcd) 511.9360 (obsd).

Table II. Summary of Crystallographic Data for $(Fe(C_5H_4PPh_2)_2)Re(CO)_3Cl$ and $(FcPPh_2)_2Re(CO)_3Cl$

	$(Fe(C_5H_4PPh_2)_2)Re(CO)_3Cl$	$(FcPPh_2)_2Re(CO)_3Cl$
empirical formula	$C_{37}H_{28}O_3P_2ClFeRe$	$C_{47}H_{38}O_3P_2ClFe_2Re$
a, Å	11.650 (2)	11.859 (2)
b, Å	19.534 (5)	20.105 (4)
c, Å	14.318 (2)	17.060 (3)
β, deg	93.76 (1)	92.26 (1)
Z	4	4
V, Å^3	3251 (2)	4064 (2)
space group	$P2_1/c$ (No. 14)	$P2_1/c$ (No. 14)
d_{calcd}, g cm^{-3}	1.757	1.709
radiation	MoKα (λ = 0.710 69 Å)	
diffractometer	Enraf-Nonius CAD-4, κ geometry	
temp, °C	23	−65
takeoff angle, deg	2.8	2.8
scan width, deg	1.00 + 0.35 tan θ	0.90 + 0.35 tan θ
scan speed, deg/min	1.2–10.0	1.2–10.0
scan type	ω	ω
data collcn range, deg	$3 \le 2\theta \le 55$	$3 \le 2\theta \le 55$
measd reflecns	*h*,*k*,±*l*	*h*,*k*,±*l*
no. of reflecns collcd	8027	10042
no. of unique data	7662	9590
averaging, R_{av}	0.028	0.059
no. of obsvd data, $I > 3\sigma(I)$	5358	5103
reflecn/param ratio	13.20	9.97
R_1[a]	0.032	0.049
R_2[b]	0.033	0.049
goodness of fit	1.09	1.11

[a] $R_1 = \sum||F_o| - |F_c||/\sum|F_o|$. [b] $R_2 = [\sum w(|F_o| - |F_c|)^2/\sum w|F_o|^2]^{1/2}$, where $w = 4F_o^2/\sigma^2(F_o^2)$; $p = 0.03$.

X-ray Crystallography. Experimental details are given in Table II. Cell constants and the orientation matrix for intensity data collection were based on the setting angle of 25 carefully centered reflections in the range $24.0 \le 2\theta \le 30.0°$. Intensity data were corrected for Lorentz and polarization effects. Neutral-atom scattering factors and anomalous dispersion effects were obtained from ref 25. All calculations for solution and refinement of the structures were performed by using TEXSAN.[26]

$(Fe(C_5H_4PPh_2)_2)Re(CO)_3Cl$. Crystals suitable for X-ray studies were grown by slow diffusion of hexane (by layering) into a solution of $(Fe(C_5H_4PPh_2)_2)Re(CO)_3Cl$ in CH_2Cl_2. An orange block crystal of approximate dimensions 0.3 × 0.3 × 0.3 mm was mounted with epoxy resin on the end of a glass fiber. Open-counter ω scans of several strong, low-angle reflections revealed structureless profiles with acceptable peak widths ($\Delta w_{1/2} = 0.25°$). Standard procedures were followed to obtain unit cell parameters and record intensity data. The space group of the crystal was uniquely determined to be $P2_1/c$ (No. 14) from systematic absences in the data.[27] The structure was solved by a combination of direct methods and standard heavy-atom Fourier techniques.[28] Full-matrix least-squares refinement was carried out on 406 variables, with anisotropic thermal parameters for the non-hydrogen atoms. Hydrogen atoms were included in calculated positions ($d_{C-H} = 0.95$ Å). An em-

(21) Tamao, K.; Kodama, S.; Nakajima, I.; Kumada, M.; Minato, A.; Suzuki, K. *Tetrahedron* **1982**, *38*, 3347–3354.
(22) Jolly, P. W.; Stone, F. G. A. *J. Chem. Soc.* **1965**, 5259–5261.
(23) Giordano, P. J.; Wrighton, M. S. *J. Am. Chem. Soc.* **1979**, *101*, 2888–2897.
(24) Haupt, H.-J.; Neumann, F.; Schwab, B.; Voigt, G. *Z. Anorg. Allg. Chem.* **1980**, *471*, 175–186.
(25) Cromer, D. T.; Waber, J. T. *International Tables for X-ray Crystallography*; Kynoch: Birmingham, England, 1974; Vol. IV. Ibers, J. A.; Hamilton, W. C. *Acta Crystallogr.* **1964**, *17*, 781–782.
(26) "TEXSAN", TEXRAY Structure Analysis Package, Molecular Structure Corp., 1985.
(27) *International Tables for X-ray Crystallography*; Hahn, T., Ed.; D. Reidel: Dordrecht, The Netherlands, 1983; Vol. A.
(28) "PHASE". Calbrese, J. C. Ph.D. Thesis, Univ of Wisconsin-Madison, 1972. "DIRDIF." Beurskens, P. T. Technical Report 1984/1, Crystallography Laboratory, Toernooiveld, 6525 Ed, Nijmigen, The Netherlands.

Table III. Final Positional and Isotropic Thermal Parameters for Non-Hydrogen Atoms in $(Fe(C_5H_4PPh_2)_2)Re(CO)_3Cl$[a]

atom	x	y	z
Re(1)	0.29568 (2)	0.12281 (1)	0.84633 (1)
Fe(1)	0.15549 (6)	0.10536 (4)	0.54639 (5)
Cl(1)	0.2500 (1)	0.23837 (7)	0.7808 (1)
P(1)	0.3994 (1)	0.08944 (7)	0.7053 (1)
P(2)	0.1047 (1)	0.08484 (7)	0.77611 (9)
O(1)	0.1947 (4)	0.1734 (3)	1.0272 (3)
O(2)	0.5206 (4)	0.1819 (3)	0.9379 (4)
O(3)	0.3441 (4)	−0.0149 (2)	0.9387 (3)
C(1)	0.2273 (5)	0.1536 (3)	0.9583 (4)
C(2)	0.4387 (5)	0.1588 (3)	0.9024 (4)
C(3)	0.3264 (5)	0.0345 (3)	0.9046 (4)
C(11)	0.3234 (4)	0.0831 (3)	0.5897 (4)
C(12)	0.3179 (5)	0.1403 (3)	0.5265 (4)
C(13)	0.2639 (5)	0.1196 (4)	0.4405 (4)
C(14)	0.2348 (5)	0.0505 (3)	0.4480 (4)
C(15)	0.2691 (4)	0.0270 (3)	0.5400 (4)
C(21)	0.4790 (4)	0.0094 (3)	0.7284 (4)
C(22)	0.4681 (5)	−0.0498 (3)	0.6756 (4)
C(23)	0.5304 (6)	−0.1081 (3)	0.7026 (5)
C(24)	0.6056 (6)	−0.1069 (3)	0.7791 (5)
C(25)	0.6212 (6)	−0.0477 (4)	0.8306 (5)
C(26)	0.5576 (5)	0.0095 (3)	0.8048 (4)
C(31)	0.5187 (4)	0.1444 (3)	0.6733 (4)
C(32)	0.6046 (5)	0.1165 (3)	0.6212 (5)
C(33)	0.6920 (5)	0.1571 (4)	0.5930 (5)
C(34)	0.6958 (5)	0.2257 (4)	0.6139 (5)
C(35)	0.6106 (5)	0.2536 (3)	0.6622 (5)
C(36)	0.5228 (5)	0.2135 (3)	0.6927 (4)
C(41)	0.0591 (4)	0.1115 (2)	0.6584 (3)
C(42)	0.0701 (5)	0.1784 (3)	0.6176 (4)
C(43)	0.0226 (5)	0.1741 (3)	0.5232 (4)
C(44)	−0.0170 (4)	0.1075 (3)	0.5056 (4)
C(45)	0.0040 (4)	0.0685 (3)	0.5877 (4)
C(51)	0.0799 (4)	−0.0079 (3)	0.7678 (3)
C(52)	−0.0290 (5)	−0.0358 (3)	0.7764 (4)
C(53)	−0.0458 (5)	−0.1056 (3)	0.7666 (4)
C(54)	0.0441 (6)	−0.1483 (3)	0.7487 (4)
C(55)	0.1528 (5)	−0.1212 (3)	0.7399 (4)
C(56)	0.1712 (4)	−0.0516 (3)	0.7504 (4)
C(61)	−0.0155 (4)	0.1108 (3)	0.8436 (3)
C(62)	−0.1060 (5)	0.1502 (3)	0.8069 (4)
C(63)	−0.1983 (5)	0.1646 (3)	0.8610 (4)
C(64)	−0.2012 (5)	0.1395 (3)	0.9497 (4)
C(65)	−0.1120 (5)	0.1011 (3)	0.9873 (4)
C(66)	−0.0180 (4)	0.0872 (3)	0.9352 (4)

[a] Numbers in parentheses refer to errors in the last digit(s). The complete atom-numbering scheme is included as supplementary material.

Table IV. Selected Interatomic Distances (Å) in $(Fe(C_5H_4PPh_2)_2)Re(CO)_3Cl$[a]

Re(1)–P(1)	2.506 (1)	O(2)–C(2)	1.144 (6)
Re(1)–P(2)	2.494 (1)	O(3)–C(3)	1.096 (6)
Re(1)–Cl(1)	2.489 (2)	Fe(1)–Cp1[b]	1.654
Re(1)–C(1)	1.932 (6)	Fe(1)–Cp2[b]	1.646
Re(1)–C(2)	1.935 (6)	C–C(Cp rings)$_{av}$	1.421 (7)
Re(1)–C(3)	1.938 (6)	C–C(phenyl rings)$_{av}$	1.381 (7)
O(1)–C(1)	1.148 (6)	Re(1)···Fe(1)	4.506 (1)

[a] See footnote *a* in Table III. [b] Cp1 = midpoint of ring C(11)–C(12)–C(13)–C(14)–C(15); Cp2 = midpoint of ring C(41)–C(42)–C(43)–C(44)–C(45).

pirical absorption correction based on ψ scans was applied. The final difference Fourier map was clean ($e < 0.8$ e Å^{-3}), and the refinement converged at $R_1 = 0.032$ and $R_2 = 0.033$. The largest parameter shift in the final cycle was 0.00σ. The final atomic positional parameters with estimated standard deviations are presented in Table III.

$(FcPPh_2)_2Re(CO)_3Cl$. Suitable crystals of $(FcPPh_2)_2Re(CO)_3Cl$ were grown by allowing a dilute solution (hexane/CH_2Cl_2, 1:1) to evaporate at room temperature. A yellow platelike crystal of approximate dimensions 0.30 × 0.25 × 0.16 mm was chosen. The crystal was mounted with epoxy resin at the tip of a glass fiber and cooled to −65 °C. Open-counter ω scans of a few low-angle intense reflections revealed somewhat broad peaks ($\Delta w_{1/2} = 0.35°$). Cell constants and the orientation matrix for intensity data collection were based on the setting angles of 25 centered reflections in the range $24.00 < 2\theta < 30.00$. The space group $P2_1/c$ (No. 14) was uniquely determined from systematic absences in the data.[26]

The Re atom was located from a Patterson map, and the remaining non-hydrogen atoms were found from subsequent difference Fourier maps. Hydrogen atoms were placed in calculated positions ($d_{C-H} = 0.95$ Å). An empirical absorption correction was applied.

The structure of $(FcPPh_2)_2Re(CO)_3Cl$ shows positional disorder between the chloride and the CO group trans to the chloride. The disorder has been adequately modeled by introducing partial occupancies in such a way that both the chloride and the carbonyl ligand are partitioned between the mutually trans sites for each. The structure refined to a 70% probability for one form over the other.

Full-matrix least-squares refinement on 512 variables allowed convergence at $R_1 = 0.049$ and $R_2 = 0.049$. All the non-hydrogen atoms, except O(3), O(3A), C(3), and C(3A), were given anisotropic thermal parameters. The hydrogen atoms were refined isotropically. The maximum parameter shift in the final cycle was 0.00σ. The final atomic positional parameters with estimated standard deviations are presented in Table VI.

Electrochemistry. Electrochemical measurements were made with a PAR Model 363 or 173 potentiostat and a Model 175 voltage programmer and were recorded on a Houston 2000 X-Y recorder. Cyclic voltammograms were measured in CH_2Cl_2/0.1 M $[n\text{-}Bu_4N]ClO_4$ for all complexes except for $(FcPy)_2Re(CO)_3Cl$, which was measured in CH_3CN/0.1 M $[n\text{-}Bu_4N]ClO_4$. More reproducible cyclic voltammograms were obtained at concentrations less than 1 mM. At complex concentrations above 1 mM, currents decreased steadily upon repetitive cycling. The reference electrode for all measurements was a Ag wire immersed in an CH_3CN solution containing 10 mM $AgNO_3$ and 0.1 M $[Et_4N]BF_4$ isolated by a frit from the remainder of the electrochemical cell. The working electrode was either a 1 mm diameter Pt disk or a 3 mm diameter glassy-carbon disk and the counter electrode was a piece of ~0.5 cm^2 Pt foil.

The number of electrons removed from a complex during an electrochemical oxidation was determined by measuring the current, i, at a rotating glassy-carbon disk electrode. Plotting log $[i/(i_d - i)]$ versus potential gives the number of electrons involved and the standard potential of the redox couple, where i_d = the diffusion-limited current.[29] This procedure yields invalid data for $(FcPPh_2)_2Re(CO)_3Cl$ because of the two closely separated redox couples (Figure 3). Measurement of a cyclic voltammogram in solution with decamethylferrocene internal standard yields the number of electrons involved in the oxidation of $(FcPPh_2)_2Re(CO)_3Cl$.

Spectroelectrochemistry. IR and UV/vis spectroelectrochemistry were conducted in a spectroelectrochemical cell described previously.[15] The electrochemical equipment was the same as that used for electrochemical measurements. CH_2Cl_2/0.1 M $[n\text{-}Bu_4N]ClO_4$ was the medium used for all complexes except for $(FcPy)_2Re(CO)_3Cl$ for which CH_3CN/0.1 M $[n\text{-}Bu_4N]ClO_4$ was used. The concentration of complexes was 5–10 mM.

In a typical experiment, the cell was purged with Ar and filled with solution, and initial IR and UV/vis spectra were measured. A cyclic voltammogram was recorded (10 mV/s) and the potential was held fixed at the potential at which the current was about half the peak current in the cyclic voltammogram. Eight to ten IR or UV/vis spectra were measured and stored electronically during the course of an electrolysis (~5–10 min) until which time the current fell to its background level and no further spectroscopic change was evident. The potential was moved 300–400 mV negative to regenerate the original species, and final IR and UV/vis spectra were taken. The peak positions in the IR spec-

Table V. Selected Angles (deg) in $(Fe(C_5H_4PPh_2)_2)Re(CO)_3Cl$[a]

P(1)–Re(1)–P(2)	93.58 (4)	Cl(1)–Re(1)–C(2)	89.1 (2)
P(1)–Re(1)–Cl(1)	91.99 (5)	Cl(1)–Re(1)–C(3)	176.3 (2)
P(2)–Re(1)–Cl(1)	87.39 (5)	C(1)–Re(1)–C(2)	86.2 (2)
P(1)–Re(1)–C(1)	174.9 (2)	C(1)–Re(1)–C(3)	89.7 (2)
P(1)–Re(1)–C(2)	88.9 (2)	C(2)–Re(1)–C(3)	90.9 (2)
P(1)–Re(1)–C(3)	91.7 (2)	O(1)–C(1)–Re(1)	174.9 (5)
P(2)–Re(1)–C(1)	91.2 (2)	O(2)–C(2)–Re(1)	177.1 (5)
P(2)–Re(1)–C(2)	175.7 (2)	O(3)–C(3)–Re(1)	178.9 (5)
P(2)–Re(1)–C(3)	92.5 (2)	Cp1[b]–Fe(1)–Cp2[b]	177.2
Cl(1)–Re(1)–C(1)	86.6 (2)	twist angle, γ[c]	14.8

[a] See footnote *a* in Table III. [b] See footnote *b* in Table IV. [c] γ = deviation from eclipsed conformation.

(29) Sawyer, D. T.; Roberts, J. L., Jr. *Experimental Electrochemistry for Chemists*; Wiley: New York, 1974; p 342.

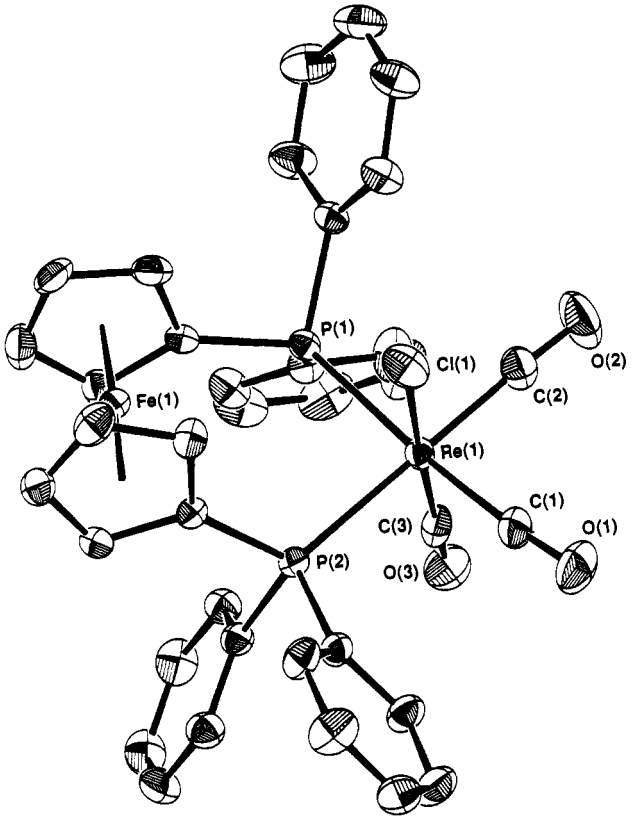

Figure 1. ORTEP view with partial atom-numbering scheme of $(Fe(C_5H_4PPh_2)_2)Re(CO)_3Cl$.

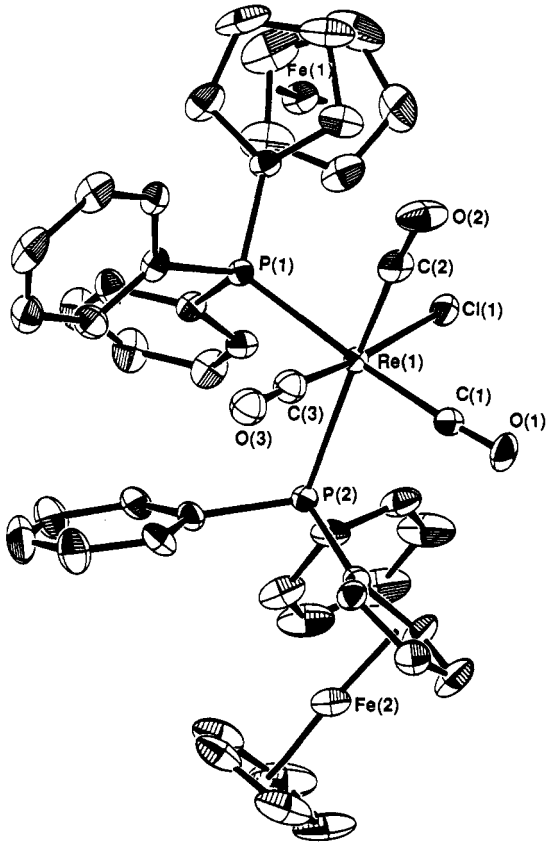

Figure 2. ORTEP view with partial atom-numbering scheme of $(FcPPh_2)_2Re(CO)_3Cl$.

trum of $(FcPPh_2)Re(CO)_3Cl^+$ were determined by subtraction of the initial spectrum of the reduced complex from the first spectrum obtained during the oxidation.

Chemical Oxidations. Chemical oxidations were conducted in CH_2Cl_2 or CH_3CN in Schlenk flasks under an atmosphere of Ar. Solutions of known concentration of the ferrocene complexes were prepared, and aliquots of known size were removed and analyzed by IR spectroscopy. A standard solution of benzoquinone and $HBF_4 \cdot Et_2O$ was prepared (typically 12 and 24 mM) in CH_2Cl_2 or CH_3CN, and a measured volume (typically 50% excess) of the oxidant was added to a solution of the metal complex. A second aliquot of known volume was removed and analyzed by IR spectroscopy, and a known volume of a standard solution of reductant ferrocene (or cobaltocene in the case of $FcRe(CO)_5$) was added to the reaction mixture. An IR spectrum of this final reaction mixture showed that 100 ± 5% of the original ferrocenyl–Re complex was obtained. The chemical oxidation of $(Fe(C_5H_4PH_2)_2)Re(CO)_3Cl$ was conducted similarly except that a standard solution of the complex was

Table VI. Final Positional and Isotropic Thermal Parameters for Non-Hydrogen Atoms in $(FcPPh_2)_2Re(CO)_3Cl$[a]

atom	*x*	*y*	*z*	*B*(eq), Å^2
Re(1)	0.25376 (3)	0.08177 (2)	0.17870 (2)	1.67 (1)
Fe(1)	0.1967 (1)	0.16310 (8)	0.46105 (8)	2.77 (7)
Fe(2)	0.2560 (1)	−0.13268 (8)	−0.02317 (9)	3.06 (7)
Cl(1)	0.0687 (5)	0.1034 (2)	0.2372 (3)	2.8 (2)
Cl(1A)	0.438 (1)	0.0730 (6)	0.1209 (6)	2.7 (5)
P(1)	0.3398 (2)	0.0763 (1)	0.3138 (1)	1.8 (1)
P(2)	0.2414 (2)	−0.0428 (1)	0.1554 (1)	1.8 (1)
O(1)	0.1499 (7)	0.1041 (4)	0.0125 (4)	3.6 (4)
O(2)	0.2913 (8)	0.2322 (4)	0.1701 (4)	4.9 (5)
O(3)	0.485 (1)	0.0668 (7)	0.1118 (8)	3.7 (4)
O(3A)	0.027 (3)	0.104 (2)	0.249 (2)	2.9 (8)
C(1)	0.1862 (9)	0.0924 (5)	0.0735 (6)	2.5 (5)
C(2)	0.276 (1)	0.1762 (6)	0.1783 (6)	3.2 (5)
C(3)	0.395 (2)	0.074 (1)	0.139 (1)	3.0 (4)
C(3A)	0.121 (4)	0.096 (2)	0.219 (2)	2.7 (8)
C(11)	0.3120 (8)	0.1463 (5)	0.3771 (5)	2.2 (4)
C(12)	0.249 (1)	0.2040 (6)	0.3602 (6)	3.5 (6)
C(13)	0.266 (1)	0.2492 (6)	0.4237 (8)	4.5 (7)
C(14)	0.337 (1)	0.2194 (8)	0.4812 (8)	5.2 (7)
C(15)	0.365 (1)	0.1558 (7)	0.4528 (6)	3.7 (6)
C(21)	0.4931 (8)	0.0777 (6)	0.3121 (5)	2.3 (4)
C(22)	0.551 (1)	0.1392 (5)	0.3166 (6)	2.7 (5)
C(23)	0.666 (1)	0.1433 (6)	0.3113 (7)	3.5 (6)
C(24)	0.7280 (8)	0.0853 (8)	0.3051 (6)	4.2 (6)
C(25)	0.676 (1)	0.0248 (7)	0.3025 (6)	3.5 (6)
C(26)	0.558 (1)	0.0211 (6)	0.3050 (6)	3.1 (5)
C(31)	0.130 (1)	0.0840 (7)	0.5185 (8)	4.9 (7)
C(32)	0.063 (1)	0.0986 (7)	0.4541 (7)	4.0 (6)
C(33)	0.024 (1)	0.1625 (8)	0.4593 (8)	4.5 (7)
C(34)	0.071 (1)	0.1904 (7)	0.530 (1)	5.6 (8)
C(35)	0.138 (1)	0.1410 (8)	0.5683 (7)	5.5 (8)
C(41)	0.3690 (8)	−0.0893 (5)	0.1889 (6)	2.4 (4)
C(42)	0.463 (1)	−0.0881 (6)	0.1439 (7)	3.5 (5)
C(43)	0.561 (1)	−0.1214 (7)	0.1691 (8)	4.7 (7)
C(44)	0.566 (1)	−0.1545 (8)	0.2363 (9)	5.3 (8)
C(45)	0.471 (1)	−0.1576 (6)	0.2817 (8)	4.8 (7)
C(46)	0.373 (1)	−0.1233 (5)	0.2597 (6)	3.1 (5)
C(51)	0.2252 (8)	−0.0551 (5)	0.0498 (6)	2.3 (4)
C(52)	0.3035 (9)	−0.0346 (5)	−0.0096 (6)	2.4 (5)
C(53)	0.246 (1)	−0.0462 (6)	−0.0841 (6)	3.3 (5)
C(54)	0.138 (1)	−0.0698 (7)	−0.0711 (6)	4.3 (6)
C(55)	0.1240 (9)	−0.0772 (7)	0.0100 (6)	3.6 (5)
C(61)	0.1221 (9)	−0.0923 (5)	0.1858 (5)	2.5 (5)
C(62)	0.129 (1)	−0.1614 (7)	0.1991 (6)	3.9 (6)
C(63)	0.036 (1)	−0.1977 (6)	0.2173 (8)	4.9 (7)
C(64)	−0.067 (1)	−0.1642 (8)	0.2256 (8)	5.8 (8)
C(65)	−0.077 (1)	−0.0973 (7)	0.2136 (8)	5.3 (8)
C(66)	0.020 (1)	−0.0613 (6)	0.1945 (6)	3.5 (5)
C(71)	0.341 (1)	−0.0720 (6)	0.4806 (6)	3.4 (5)
C(72)	0.235 (1)	−0.0987 (6)	0.4665 (6)	3.6 (6)
C(73)	0.1659 (9)	−0.0760 (6)	0.4092 (6)	3.2 (5)
C(74)	0.1999 (9)	−0.0226 (5)	0.3629 (5)	2.2 (4)
C(75)	0.3055 (8)	0.0038 (5)	0.3737 (5)	2.2 (4)
C(76)	0.375 (1)	−0.0198 (6)	0.4330 (6)	3.1 (5)
C(81)	0.336 (1)	−0.1972 (7)	−0.0944 (8)	5.7 (8)
C(82)	0.225 (2)	−0.2222 (7)	−0.078 (1)	7 (1)
C(83)	0.397 (1)	−0.1915 (6)	−0.0226 (8)	4.5 (7)
C(84)	0.223 (2)	−0.2294 (7)	0.006 (1)	7 (1)
C(85)	0.329 (1)	−0.2100 (6)	0.0373 (8)	4.9 (7)

[a] Numbers in parentheses refer to errors in the last digit(s). A complete atom-numbering scheme is included as supplementary material.

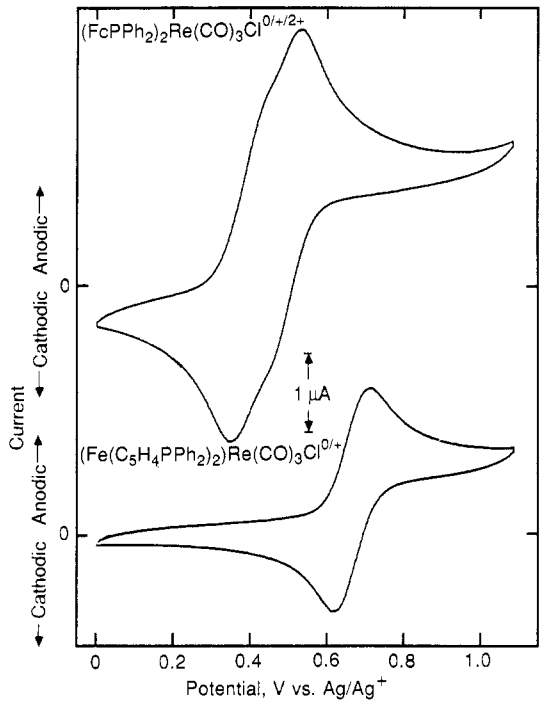

Figure 3. Cyclic voltammograms for the complexes indicated measured at 100 mV/s in CH_2Cl_2/0.1 M [*n*-Bu_4N]ClO_4 at a Pt electrode at 25 °C.

added to a known (typically a 50% excess here also) quantity of $NOBF_4$. IR spectra were recorded before and after oxidation and after reduction with ferrocene as above.

Results and Discussion

Synthesis of Ferrocenyl–Rhenium Complexes. We prepared the new ligand 4-ferrocenylpyridine by nickel-catalyzed coupling of the Grignard reagent from bromoferrocene with 4-bromopyridine. The complexes of rhenium shown in Scheme I containing bis(diphenylphosphino)ferrocene, diphenylferrocenylphosphine, and 4-ferrocenylpyridine were prepared by simple substitution reactions on $Re(CO)_5Cl$ in $CHCl_3$ or toluene. Details of the procedures are give in the Experimental Section. Each of these reaction proceeds in high yield, providing yellow, crystalline, high-melting solids. The complexes were characterized by a combination of IR, UV/vis, ^1H, ^{13}C, and ^{31}P NMR, and mass spectroscopies, X-ray crystallography, and elemental analysis. Some relevant spectroscopic data are given in Table I and in the Experimental Section.

We base the cis assignment in $(FcPPh_2)Re(CO)_4Cl$ on the positions and intensities of the Re–CO bands in the IR spectrum. They are nearly identical with those for *cis*-$(PPh_3)Re(CO)_4Cl$.[22] The structures of $(Fe(\eta^5\text{-}C_5H_4PPh_2)_2)Re(CO)_3Cl$ and $(FcPPh_2)_2Re(CO)_3Cl$ were determined unambiguously by X-ray crystallography (vide infra). The assignment of the *fac* structure to $(FcPy)_2Re(CO)_3Cl$ is based on the Re–CO bands in the IR spectrum and the observation that the ^1H NMR and ^{13}C NMR parameters are identical for the pyridine ligands. The three-band pattern observed in the CO stretching region of the IR spectrum is typical for *fac*-$L_2Re(CO)_3Cl$ complexes.[15,22,23]

We examined two synthetic routes to $FcRe(CO)_5$. Reaction of $NaRe(CO)_5$ with ferrocenecarbonyl chloride provided mainly $Re_2(CO)_{10}$ and a small quantity of the desired $(\eta^5\text{-}C_5H_5)(\eta^5\text{-}C_5H_4CORe(CO)_5)Fe$. Thermal decarbonylation in toluene gives $FcRe(CO)_5$ in low yield. Photolysis (254 nm) of Ph_2Hg in the presence of $Re_2(CO)_{10}$ has been shown to yield $PhRe(CO)_5$ in moderate yields.[24] Photolysis (254 nm) of Fc_2Hg and $Re_2(CO)_{10}$ in C_6H_6 gives $FcRe(CO)_5$ in low but acceptable yields.

Solid-State Structures. Structural studies on transition-metal complexes of $Fe(C_5H_4PPh_2)_2$ have been reported for $(Fe(C_5H_4PPh_2)_2)Rh(norbornadiene)^+$,[30] $(Fe(C_5H_4PPh_2)_2)PtCl_2$,[31] $(Fe(C_5H_4PPh_2)_2)PdCl_2$·solvent,[32,33] $Fe(C_5H_4PPh_2)_2)NiBr_2$,[32] $(Fe(C_5H_4PPh_2)_2)(MeCp)Mn(CO)$,[34] and $(Fe(C_5H_4PPh_2)_2)Mo(CO)_4$.[32] The bis(phosphine) ligand in the above complexes is bonded in a bidentate fashion to the metal atoms. The cyclopentadienyl rings of the ferrocene moiety exhibit staggered conformations in the square planar Rh, Pt, and Pd complexes and in the octahedral Mo complex. An eclipsed conformation of the rings is observed for the tetrahedral Ni and Mn complexes.

In our study, $(Fe(C_5H_4PPh_2)_2)Re(CO)_3Cl$ demonstrates nearly idealized octahedral geometry for Re, and the cyclopentadienyl rings in the bidentate phosphine are staggered (deviation from eclipsed conformation is 15°). Pertinent bond distances and angles are given in Tables IV and V, respectively. An ORTEP view, with partial atom-numbering scheme, is shown in Figure 1. The structure reveals a facial arrangement for the carbonyl groups, consistent with the structural assignment from IR studies. The P(1)–Re(1)–P(2) angle of 93.58 (4)° is slightly larger than the ideal value, although much larger deviation has been observed in the square-planar $(Fe(C_5H_4PPh_2)_2)PtCl_2$ (P–Pt–P = 99.3 (1)°) and $(Fe(C_5H_4PPh_2)_2)PdCl_2$ (P–Pd–P = 97.98 (4)°) complexes. Remaining interatomic distances and angles in the molecule are normal. Separation between Fe(1) and Re(1) in $(Fe(C_5H_4PPh_2)_2)Re(CO)_3Cl$ is 4.506 (1) Å, which is too long for any significant metal–metal interaction to exist between the two atoms.

The complex $(FcPPh_2)_2Re(CO)_3Cl$ is one of two complexes of $FcPPh_2$ that have recently been structurally characterized in our laboratory.[35] An ORTEP drawing of $(FcPPh_2)_2Re(CO)_3Cl$ is shown

Table VII. Selected Interatomic Distances (Å) in $(FcPPh_2)_2Re(CO)_3Cl$[a]

Re(1)–P(1)	2.486 (2)	P(2)–C(61)	1.82 (1)
Re(1)–P(2)	2.539 (3)	P(2)–C(41)	1.85 (1)
Re(1)–Cl(1)	2.485 (6)	O(1)–C(1)	1.14 (1)
Re(1)–Cl(1A)	2.44 (1)	O(2)–C(2)	1.15 (1)
Re(1)–C(1)	1.95 (1)	O(3)–C(3)	1.19 (2)
Re(1)–C(2)	1.92 (1)	O(3A)–C(3A)	1.25 (4)
Re(1)–C(3)	1.84 (2)	C–C(Cp ring)$_{av}$	1.41 (1)
Re(1)–C(3A)	1.76 (4)	C–C(phenyl rings)$_{av}$	1.38 (1)
Fe(1)–C(ring)$_{av}$	2.03 (1)	Re(1)···Fe(1)	5.157 (2)
Fe(2)–C(ring)$_{av}$	2.04 (1)	Re(1)···Fe(2)	5.519 (2)
P(1)–C(11)	1.81 (1)	Fe(1)–Cp1[b]	1.634
P(1)–C(21)	1.82 (1)	Fe(1)–Cp2[b]	1.652
P(1)–C(75)	1.84 (1)	Fe(2)–Cp3[b]	1.636
P(2)–C(51)	1.82 (1)	Fe(2)–Cp4[b]	1.655

[a] See footnote *a* in Table VI. [b] Cp1 = midpoint of ring C(11)–C(12)–C(13)–C(14)–C(15); Cp2 = midpoint of ring C(31)–C(32)–C(33)–C(34)–C(35); Cp3 = midpoint of ring C(51)–C(52)–C(53)–C(54)–C(55); Cp4 = midpoint of ring C(81)–C(82)–C(83)–C(84)–C(85).

Table VIII. Selected Angles (deg) in $(FcPPh_2)_2Re(CO)_3Cl$[a]

P(1)–Re(1)–P(2)	96.92 (8)	C(3)–Re(1)–Cl(1)	174.2 (7)
Cl(1)–Re(1)–P(1)	88.4 (1)	C(1)–Re(1)–C(2)	86.5 (4)
Cl(1)–Re(1)–P(2)	100.9 (1)	C(1)–Re(1)–C(3)	91.3 (6)
C(1)–Re(1)–P(1)	176.2 (3)	C(2)–Re(1)–C(3)	87.6 (8)
C(1)–Re(1)–P(2)	86.9 (3)	O(1)–C(1)–Re(1)	174 (1)
C(1)–Re(1)–Cl(1)	90.8 (3)	O(2)–C(2)–Re(1)	173 (1)
C(2)–Re(1)–P(1)	89.8 (3)	O(3)–C(3)–Re(1)	177 (2)
C(2)–Re(1)–P(2)	169.7 (3)	Cp1[b]–Fe(1)–Cp2[b]	176.6
C(2)–Re(1)–Cl(1)	87.1 (4)	Cp3[b]–Fe(2)–Cp4[b]	176.8
C(3)–Re(1)–P(1)	89.2 (6)	twist angle, γ	20.4[c]
C(3)–Re(1)–P(2)	84.6 (7)		1.9[d]

[a] See footnote *a* in Table VI. [b] See footnote *b* in Table VII. [c] Twist angle between Cp1 and Cp2. [d] Twist angle between Cp3 and Cp4.

(30) Cullen, W. R.; Kim, T.; Einstein, F. W. B.; Jones, T. *Organometallics* **1985**, *4*, 346–351.
(31) Clemente, D. A.; Pilloni, G.; Corain, B.; Longato, B.; Tripicchio-Camellini, M. *Inorg. Chim. Acta* **1986**, *115*, L9–L11.
(32) Butler, I. R.; Cullen, W. R.; Kim, T.; Rettig, S. J.; Trotter, J. *Organometallics* **1985**, *4*, 972–980.
(33) Hayashi, T.; Konishi, M.; Kobori, Y.; Kumada, M.; Higuchi, T.; Hirotsu, K. *J. Am. Chem. Soc.* **1984**, *106*, 158–163.
(34) Onaka, S. *Bull. Chem. Soc. Jpn.* **1986**, *59*, 2359–2361.

Table IX. $E_{1/2}$ Values and Number of Electrons Removed in Oxidations of Ferrocenyl–Rhenium Complexes[a]

complex	$E_{1/2}$, V vs Ag/Ag^+	no. of e
ferrocene	0.26	
$FcRe(CO)_5$	0.01	0.97
$Fe(C_5H_4PPh_2)_2$	0.53[b]	
$(Fe(C_5H_4PPh_2)_2)Re(CO)_3Cl$	0.67	1.0
$FcPPh_2$	0.40	
$(FcPPh_2)Re(CO)_4Cl$	0.43	0.96
$(FcPPh_2)_2Re(CO)_3Cl$	0.42, 0.52	1.8
4-ferrocenylpyridine	0.36	
$(FcPy)_2Re(CO)_3Cl$	0.37[c]	2.1
$(dppe)Re(CO)_3Cl$[d]	1.4[b]	

[a] The values of $E_{1/2}$ and the number of electrons removed were determined in CH_2Cl_2/0.1 M $[n\text{-}Bu_4N]ClO_4$ unless noted otherwise. The values of $E_{1/2}$ are the average of the potentials for peak anodic and cathodic currents in the cyclic voltammograms recorded at 100 mV/s. [b] These complexes oxidize irreversibly, and the values reported are the positions of peak anodic currents. [c] The values of $E_{1/2}$ and the number of electrons removed were determined in CH_3CN/0.1 M $[n\text{-}Bu_4N]ClO_4$. [d] dppe = bis(diphenylphosphino)ethane.

in Figure 2. Selected bond distances and angles are given in Tables VII and VIII, respectively. Like $(Fe(C_5H_4PPh_2)_2)Re(CO)_3Cl$, $(FcPPh_2)_2Re(CO)_3Cl$ also has a facial arrangement of carbonyl groups. The presence of positional disorder between C(3)–O(3) and Cl(1) was a disturbing feature during solution of the structure, although we were able to model the disorder adequately, and normal bond lengths and angles have been obtained for the disordered atoms.

Considerable deviation from idealized octahedral geometry around Re is observed in $(FcPPh_2)_2Re(CO)_3Cl$. Notable examples are Cl(1)–Re(1)–P(2) and C(2)–Re(1)–P(2) angles of 100.9 (1)° and 169.7 (3)°, respectively. These distortions are possibly due to steric crowding imposed by the ferrocenyl groups. The Re(1)–P(2) distance is slightly longer than the Re(1)–P(1) distance. The cyclopentadienyl rings attached to Fe(1) are staggered (twist angle = 20°), but a nearly eclipsed conformation (twist angle = 2°) is seen for the cyclopentadienyl rings attached to Fe(2). We should note that a similar eclipsed conformation for the cyclopentadienyl rings is found in *trans*-$Ir(CO)Cl(FcPPh_2)_2$.[34] The Fe–Re separations in $(FcPPh_2)_2Re(CO)_3Cl$ are 5.157 (2) Å (Re(1)···Fe(1)) and 5.519 (2) Å (Re(1)···Fe(2)) and, as in $(Fe(C_5H_4PPh_2)_2)Re(CO)_3Cl$, metal–metal interaction is very unlikely.

Electrochemistry of Ferrocenyl–Rhenium Complexes. All five Re complexes illustrated in Scheme I show reversible oxidations at Pt or glassy-carbon electrodes in CH_2Cl_2/0.1 M $[n\text{-}Bu_4N]ClO_4$ solution. Figure 3 shows representative cyclic voltammograms, and Table IX summarizes half-wave potentials, $E_{1/2}$, and the number of electrons removed in the oxidations of the complexes. Also shown in Table IX are the $E_{1/2}$ values for the free ligands: bis(diphenylphosphino)ferrocene, diphenylferrocenylphosphine, and 4-ferrocenylpyridine. Small positive shifts in $E_{1/2}$ values are observed upon coordination of these ligands to Re. The oxidation potential of $(dppe)Re(CO)_3Cl$ (dppe = bis(diphenylphosphino)ethane) is included to demonstrate that the Re center is not oxidized at potentials where the ferrocenyl-based oxidations occur. No clear second or third oxidation wave associated with Re is observed for any of the ferrocenyl–Re complexes when the potential is scanned to the positive solvent limit (~1.5 V).

The cyclic voltammogram of the complex $(FcPPh_2)_2Re(CO)_3Cl$ has two anodic and cathodic waves separated by ~100 mV (Figure 3). The small separation of the first and second oxidation signals small, but significant, electronic interaction between the two ferrocenyl ligands. This interaction is analogous to the interaction in various linked metallocenes.[36] In contrast, the cyclic voltammograms of the complex $(FcPy)_2Re(CO)_3Cl$ contains only one two-electron-oxidation wave revealing very little ferrocenyl–ferrocenyl electronic coupling. The −250-mV shift in $E_{1/2}$ upon substitution of $Re(CO)_5$ for hydrogen in ferrocene is remarkable and represents the largest "substituent" effect observed in the cyclic voltammetry studies. It is noteworthy that substitution of $-CH_3$ for H in ferrocene only shifts $E_{1/2}$ by ~50 mV. The effect of introducing $-Re(CO)_5$ is equivalent to replacing five H's of ferrocene with five $-CH_3$ groups!

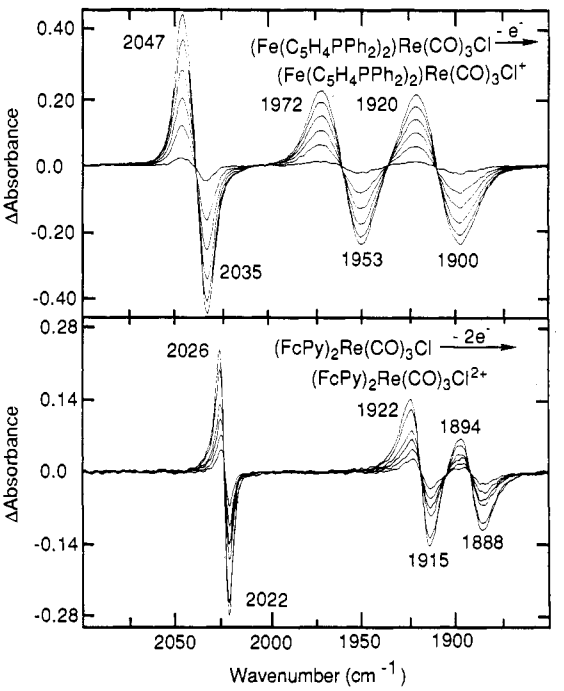

Figure 4. IR difference spectra accompanying oxidation of ferrocenyl–rhenium complexes in CH_2Cl_2/0.1 M $[n\text{-}Bu_4N]ClO_4$ for $(Fe(C_5H_4PPh_2)_2)Re(CO)_3Cl$ and in CH_3CN/0.1 M $[n\text{-}Bu_4N]ClO_4$ for $(FcPy)_2Re(CO)_3Cl$.

Table X. Shifts Observed in the Carbonyl Stretching Frequencies upon Oxidation of Ferrocenyl–Rhenium Complexes[a]

complex	change in peak position, cm^{-1} A′(cis)	A″(cis)	A′(trans)
$(Fe(C_5H_4PPh_2)_2)Re(CO)_3Cl$	12	19	20
$(FcPPh_2)_2Re(CO)_3Cl$ (1 e)	5	5	9
(2 e)	8	10	16
$(FcPy)_2Re(CO)_3Cl$ (2 e)	4	7	6

	change in peak position, cm^{-1} ν_1	ν_2	ν_3	ν_4
$FcRe(CO)_5$	12	27	14	33
$(FcPPh_2)Re(CO)_4Cl$	3	11	2	20

[a] The ν_1 values are for the highest energy band in the IR spectrum and all of the shifts are to higher wavenumbers.

Spectroelectrochemistry of Ferrocenyl–Rhenium Complexes. UV/vis and IR spectroelectrochemistry were carried out in a cell composed of Pt-gauze working and counter electrodes and a Ag quasi-reference electrode sandwiched between two NaCl crystals.[15] The crystals were separated by approximately 0.2 mm. Spectra were taken only of the region surrounding the working electrode.

Figure 4 shows IR difference spectra in the Re–CO region accompanying oxidations of $(Fe(C_5H_4PPh_2)_2)Re(CO)_3Cl$ and $(FcPy)_2Re(CO)_3Cl$. The negative peaks correspond to the disappearance of the starting reduced complexes and positive peaks correspond to appearance of oxidized complexes. The patterns of bands in the IR for oxidized complexes are qualitatively similar to those for the reduced complexes. However, all peaks for the oxidized complexes are shifted to higher energy compared to those for the reduced species. The similarity of the pattern of CO stretching bands for oxidized and reduced complexes indicates

(35) The other structurally characterized complex is *trans*-$Ir(CO)Cl(FcPPh_2)_2$. The structure will be published elsewhere. Ahmed, K. J.; Davis, W.; Wrighton, M. S. Manuscript in preparation.

(36) Levanda, C.; Bechgaard, K.; Cowan, D. O. *J. Org. Chem.* **1976**, *41*, 2700–2704.

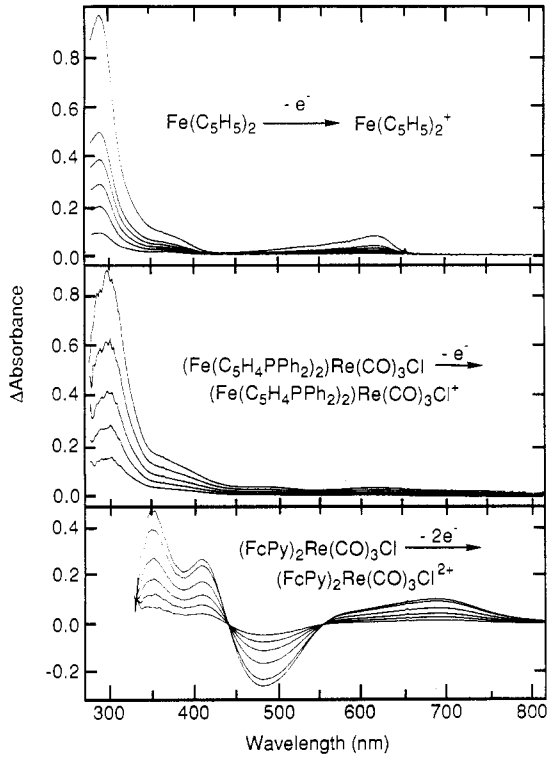

Figure 5. UV/vis difference spectra accompanying oxidation of ferrocene and ferrocenyl–rhenium complexes. The spectra for ferrocene and $(Fe(C_5H_4PPh_2)_2)Re(CO)_3Cl$ were measured in CH_2Cl_2/0.1 M $[n\text{-}Bu_4N]ClO_4$ and those for $(FcPy)_2Re(CO)_3Cl$ were measured in CH_3CN/0.1 M $[n\text{-}Bu_4N]ClO_4$.

that major structural rearrangements do not accompany oxidation. All five complexes examined show shifts of the CO bands to higher energies upon oxidation. Table I includes IR data for reduced and oxidized species, and Table X summarizes shifts in peak positions observed.

Figure 5 shows UV/vis difference spectra accompanying oxidations of ferrocene, $(Fe(C_5H_4PPh_2)_2)Re(CO)_3Cl$, and $(FcPy)_2Re(CO)_3Cl$. The bands that appear in the oxidation of the two Re complexes are similar to those observed in the oxidation of ferrocene itself. All of the oxidized complexes except for $(Fe(C_5H_4PPh_2)_2)Re(CO)_3Cl^+$ have a band in the visible region between 600 and 710 nm having a molar absorptivity of 400–700 M^{-1} cm^{-1}, which is characteristic of the ferrocenium ion (617 nm, ϵ = 450 M^{-1} cm^{-1}).[37] The complex $(Fe(C_5H_4PPh_2)_2)Re(CO)_3Cl^+$ has a band at 620 nm, but its molar absorptivity is only 150 M^{-1} cm^{-1}. Table I includes UV/vis spectral data for reduced and oxidized species.

Several points concerning the IR and UV/vis spectroelectrochemistry deserve further comment. First, the changes in the IR and UV/vis spectra are completely reversible except those for the complex $(FcPPh_2)_2Re(CO)_3Cl$. Greater than 94% of the original absorbances in the IR region for the reduced complexes is recovered upon bringing the potential negative. The complex $(FcPPh_2)_2Re(CO)_3Cl$ is unstable when oxidized by two electrons during a spectroelectrochemical experiment, and only about 75% of this complex is recovered upon reduction. We have not identified the decomposition product(s). Second, the shifts in the IR spectra are independent of the counter ion; studies have been carried out with $[n\text{-}Bu_4N]^+PF_6^-$, BF_4^-, and ClO_4^-.

Third, the magnitude of the shifts in the Re–CO peak positions upon oxidation depends upon the number of bonds between the ferrocenyl group and the Re, the number of ferrocenyl groups in the complex, and the number of connections between the ferrocenyl unit and the Re. The complex having the largest single shift and the largest total shift in carbonyl stretching frequency, $FcRe(CO)_5$, has a direct σ-bond between the ferrocenyl group and Re. Oxidation of $(FcPy)_2Re(CO)_3Cl$ results in the smallest change in peak positions of the complexes studied. One-electron oxidation of $(Fe(C_5H_4PPh_2)_2)Re(CO)_3Cl$ results in larger shifts in peak position than are observed on one- or two-electron oxidation of $(FcPPh_2)_2Re(CO)_3Cl$. The bidentate chelate clearly interacts more strongly than do the monodentate ligands. Curiously, oxidation of one ferrocenyl unit in $(FcPPh_2)Re(CO)_4Cl$ results in larger shifts in peak positions than oxidation of both ferrocenyl units in $(FcPPh_2)_2Re(CO)_3Cl$, but it is difficult to interpret small differences among complexes of different geometry. Consistent with expectation, oxidation of both ferrocenyl groups in $(FcPPh_2)_2Re(CO)_3Cl$ causes a larger shift than oxidation of only one.

Fourth, it is of interest to compare the shifts observed upon oxidation of ferrocenyl units in $(FcPy)_2Re(CO)_3Cl$ to the changes in peak positions of the Re–CO bands in $(4\text{-X-py})_2Re(CO)_3Cl$ (X = H, Ph, PhCO, CN) as a function of X.[23,38] Substitution of PhCO for H shifts the bands from 2027, 1922, and 1886 cm^{-1} to 2031, 1929, and 1894 cm^{-1}. The magnitude of these changes is very similar to the changes resulting from one-electron oxidation of each ferrocenyl unit in $(FcPy)_2Re(CO)_3Cl$, Tables I and X. Substitution of CN for H causes larger shifts to 2032, 1936, and 1898 cm^{-1}, and substitution of Ph for H causes insignificant shifts.

Fifth, it is interesting to observe the consequences of oxidation of the ferrocenes in $(FcPy)_2Re(CO)_3Cl$ in the UV/vis spectrum. We have examined UV/vis spectroelectrochemistry of $(FePy)_2Re(CO)_3Cl$ at lower concentrations than that shown in Figure 5 in which the data at shorter wavelengths are usable. $(FcPy)_2Re(CO)_3Cl$ has a strong Re-to-pyridine charge-transfer band at 306 nm as do other $(4\text{-X-py})_2Re(CO)_3Cl$ complexes.[23] Oxidation of the ferrocene increases the electron-withdrawing ability of the ligand and should cause the Re-to-pyridine charge-transfer band to shift to lower energy. A new band appears at ~350 nm in the spectrum of $(FcPy)_2Re(CO)_3Cl^{2+}$ which may be attributable to a shifted Re-to-pyridine charge transfer absorption; however, this new band is significantly less intense than the band at 305 nm in the spectrum of $(FcPy)_2Re(CO)_3Cl$ and its assignment is unclear.

Finally, the positions of the ferrocenium bands in the UV/vis spectra of the oxidized ferrocenyl–rhenium complexes merit comment. $FcRe(CO)_5$ and $(FcPy)_2Re(CO)_3Cl$ have the lowest oxidation potentials and upon oxidation have the lowest absorption bands red shifted in comparison with the first absorption of ferrocenium. This shift presumably arises because this band is a ligand-to-Fe(III) absorption and the "ligand" orbitals are raised in energy in comparison to ferrocenium itself. The similarity of the band positions for the remaining ferrocenyl–rhenium complexes to that of ferrocenium suggests that these substituted ferrocenium derivatives are not substantially altered with respect to the energetics for the ligand-to-Fe(III) charge transfer.

Chemical Oxidation of the Ferrocenyl–Rhenium Complexes. Benzoquinone (0.5 equiv/equiv of Fe) and $HBF_4{\cdot}Et_2O$ (1.0 equiv/equiv of Fe) in CH_2Cl_2 or in CH_3CN for $(FcPy)_2Re(CO)_3Cl$ effect oxidation of $FcRe(CO)_5$, $(FcPy)_2Re(CO)_3Cl$, $(FcPPh_2)Re(CO)_4Cl$, and $(FcPPh_2)_2Re(CO)_3Cl$, as deduced from IR and UV/vis spectral changes. The complex $(FcPy)_2Re(CO)_3Cl^{2+}$ is insoluble in CH_2Cl_2. In general, a 50% excess of oxidant was used to assure complete oxidation of the complexes. Stoichiometric oxidations are in qualitative accord with the electrochemical determination of the number of electrons removed. The chemical oxidations proceed on the time scale of mixing, giving blue-green homogeneous solutions. IR spectra of these solutions show complete loss of the neutral complexes and growth of bands at higher energies due to the oxidized complexes. The peak positions of the oxidized complexes produced electrochemically and chemically differ by less than 1–2 cm^{-1}. Attempted oxidation of $(Fe(C_5H_4PPh_2)_2)Re(CO)_3Cl$ with benzoquinone/$HBF_4{\cdot}Et_2O$ (0.75 equiv/1.5 equiv) resulted in oxidation of only

(37) Sohn, Y. S.; Hendrickson, D. N.; Gray, H. B. *J. Am. Chem. Soc.* **1971**, *93*, 3603–3612.

(38) Giordano, P. J. Ph.D. Thesis, Massachusetts Institute of Technology, 1976.

~10% of the oxidized complex. The powerful one-electron-oxidants $NOBF_4$, $NOPF_6$, or NO_2BF_4 effect the complete oxidation of $(Fe(C_5H_4PPh_2)_2)Re(CO)_3Cl$ within 1-2 h in CH_2Cl_2. The slow rate of these oxidations is probably caused by the insolubility of the oxidizing agents in CH_2Cl_2. Chemically produced $(FcPPh_2)_2Re(CO)_3Cl^{2+}$ is also unstable and decomposes, yielding some $(FcPPh_2)Re(CO)_4Cl$.

The chemically oxidized complexes can, in all cases, be chemically reduced back to the neutral complexes by addition of ferrocene or cobaltocene in the case of $FcRe(CO)_5$. We investigated these oxidation and reductions quantitatively by IR spectroscopy and found that in all cases the reduced complexes could be recovered in greater than 95% yield. Even $(FcPPh_2)_2Re(CO)_3Cl$ could be chemically oxidized and reduced before significant decomposition occurred. The quantitative nature of these redox reactions permits determination of IR molar absorptivities for the oxidized complexes. These values are reported in Table I. Values obtained for IR molar absorptivities in spectroelectrochemical experiments by assuming quantitative production of oxidized complex are in reasonable (±20%) agreement. The concomitant reduction of benzoquinone to hydroquinone accompanying chemical oxidation of ferrocenyl complexes make determination of UV/vis extinction coefficients from spectra of chemically oxidized complexes difficult. We measured the UV/vis spectrum of chemically oxidized $(Fe(C_5H_4PPh_2)_2)Re(CO)_3Cl$ since the byproduct, NO, is gaseous, and it is in good agreement with the spectrum obtained in the spectroelectrochemical cell.

Conclusions

The five Re complexes containing ferrocenyl ligands shown in Scheme I have been synthesized and characterized. In each of the complexes the ferrocenyl unit(s) can be reversibly oxidized by one electron each. That the oxidation is ferrocenyl-centered is supported by the oxidation potentials of the free ligands and the observation of bands in the UV/vis similar to those for ferrocenium. The oxidized complexes have been characterized spectroscopically (IR and UV/vis) and chemically by reduction back to their neutral complexes. Peak positions in the CO stretching region of the IR spectra all shift to higher energy upon oxidation of the complexes. The shift of the Re–CO peak positions to higher energy is indicative of lowered electron density at the Re atom. The magnitude of the shift depends upon the distance or the number of bonds separating the Re atom and ferrocenyl moiety. The important point of this work is that electron density at a metal center can be predictably adjusted by oxidation of a pendant redox center.

Tuning the electron density at a metal center by oxidation of a pendant ferrocene represents a new and useful alternative to tuning by varying the substituents on cyclopentadienyl or pyridyl ligands or reduction of pendant redox ligands. Work in this laboratory is in progress to examine the effect of the oxidation state of a pendant redox ligand upon the rate or equilibrium constant of a reaction at the effected metal center and to design other redox-active ligands.

Acknowledgment. We thank Dr. William Davis, Staff Crystallographer, Department of Chemistry, MIT, for collecting the X-ray crystallographic data and providing assistance with the structure solutions. We thank the National Science Foundation for support of this research.

Registry No. $FcPy^+$, 120577-84-6; FcPy, 120577-85-7; Fc, 102-54-5; Fc^+, 12125-80-3; $(dppe)Re(CO)_3Cl$, 25257-38-9; $Re(CO)_5Cl$, 14099-01-5; *fac*-$(Fe(C_5H_4PPh_2)_2)Re(CO)_3Cl$, 120577-73-3; *fac*-$(FcPy)_2Re(CO)_3Cl$, 120577-74-4; *cis*-$(FcPPh_2)Re(CO)_4Cl$, 120577-75-5; *fac*-$(FcPPh_2)_2Re(CO)_3Cl$, 120577-76-6; $FcPPh_2$, 12098-17-8; $FcRe(CO)_5$, 120577-77-7; $FcRe(CO)_5^+$, 120577-78-8; *fac*-$(Fe(C_5H_4PPh_2)_2)Re(CO)_3Cl^+$, 120577-79-9; *cis*-$(FcPPh_2)Re(CO)_4Cl^+$, 120608-47-1; *fac*-$(FcPy)_2Re(CO)_3Cl^{2+}$, 120577-80-2; *fac*-$(FcPPh_2)_2Re(CO)_3Cl^{2+}$, 120577-81-3; *fac*-$(FcPPh_2)_2Re(CO)_3Cl^+$, 120577-82-4; $Fe(C_5H_4PPh_2)_2$, 12150-46-8; $FcPPh_2^+$, 120577-83-5; FcBr, 1273-73-0; Fc_2Hg, 1274-09-5; 1,2-dibromoethane, 106-93-4; 4-bromopyridine, 1120-87-2; *cis*-(1,3-bis(diphenylphosphino)propane)dichloronickel, 55659-60-4.

Supplementary Material Available: Complete atom-labeling scheme (Figure S1) and complete listings of bond lengths and angles (Table S1), anisotropic thermal parameters for non-hydrogen atoms and isotropic thermal parameters for the hydrogen atoms (Table S2), and hydrogen atom coordinates (Table S3) for $(Fe(C_5H_4PPh_2)_2)Re(CO)_3Cl$ and complete atom-labeling scheme (Figure S2) and complete listings of bond lengths and angles (Table S5), anisotropic thermal parameters for non-hydrogen atoms and isotropic thermal parameters for the hydrogen atoms (Table S6), and hydrogen atom coordinates (Table S7) for $(FePPh_2)_2Re(CO)_3Cl$ (16 pages); listings of F_o and F_c for both compounds (Tables S4 and S8) (57 pages). Ordering information is given on any current masthead page.

Contribution from the General Electric Company, Silicone Products Division,[1] 1 Hudson River Road, Waterford, New York 12188

Asymmetric Distannoxane Dimers

David C. Gross

Received September 29, 1988

Solutions of difunctional tetrabutyldistannoxane pairs containing identical and mixed substitutions, $[Bu_2SnX]_2O$ plus $XBu_2SnOSnBu_2Y$ (X, Y = CH_3CO_2, Cl, CH_3O, C_6H_5O), respectively, were examined by ^{119}Sn NMR spectroscopy. In all cases, the resulting eight-line spectra suggest that the two starting compounds are in equilibrium with the three possible distannoxane dimers. Each dimer is associated in a "ladder" or "staircase" geometry; the mixed species comprise four chemically nonequivalent tin atoms. In contrast, there was, with one exception (X = Cl, Y = $MeCO_2$), no spectral evidence for the stable formation of dimers formed from a pair of symmetrically disubstituted species, $\{[Bu_2SnX]_2O\cdot[Bu_2SnY]_2O\}$. An irreversible ligand conproportionation reaction of the two compounds resulted in the quantitative formation of 2 equiv of $XBu_2SnOSnBu_2Y$.

Introduction

Condensed organotin species, particularly the tetraalkyldistannoxanes, are well-known moisture cure catalysts for room-temperature-vulcanized (RTV) silicone elastomers.[2] Each year in fact, organotin reagents such as these are utilized to cross-link literally tons of linear siloxane polymer. This report presents ^{119}Sn NMR data that can be employed to successfully identify the composition and structure of a mixture of active silicone RTV cure catalysts in solution. The NMR data has additional significance in light of recent reports by Otera et al. describing the use of distannoxanes as catalysts for urethane polymerization[3] and

(1) Initial experiments were conducted at the General Electric Corporate Research and Development Center, 1 River Road, Schenectady, NY 12345.

(2) Chadha, R. J; Panda, K. C. U.S. Pat. 3,664,997.

(3) Otera, J.; Yano, T.; Okawara, R. *Organometallics* **1986**, *5*, 1167.

0020-1669/89/1328-2355$01.50/0